

Bias-dependent conductive characteristics of individual GeSi quantum dots studied by conductive atomic force microscopy

This article has been downloaded from IOPscience. Please scroll down to see the full text article.

2011 Nanotechnology 22 095708

(<http://iopscience.iop.org/0957-4484/22/9/095708>)

View [the table of contents for this issue](#), or go to the [journal homepage](#) for more

Download details:

IP Address: 130.209.6.41

The article was downloaded on 05/04/2012 at 17:57

Please note that [terms and conditions apply](#).

Bias-dependent conductive characteristics of individual GeSi quantum dots studied by conductive atomic force microscopy

R Wu^{1,2}, S L Zhang¹, J H Lin¹, Z M Jiang¹ and X J Yang^{1,3}

¹ State Key Laboratory of Surface Physics, Fudan University, Shanghai 200433, People's Republic of China

² School of Physics Science and Technology, Xinjiang University, Urumqi, Xinjiang 830046, People's Republic of China

E-mail: xjyang@fudan.edu.cn

Received 18 November 2010, in final form 22 December 2010

Published 27 January 2011

Online at stacks.iop.org/Nano/22/095708

Abstract

The bias-dependent electrical characteristics of individual self-assembled GeSi quantum dots (QDs) are investigated by conductive atomic force microscopy. The results reveal that the conductive characteristics of QDs are strongly influenced by the applied bias. At low (-0.5 to -2.0 V) and high (-2.5 to -4.0 V) biases, the current distributions of individual GeSi QDs exhibit ring-like and disc-like characteristics respectively. The current of the QD's central part increases more quickly than that of the other parts as the bias magnitude increases. Histograms of the magnitude of the current on a number of QDs exhibit the same single-peak feature at low biases, and double- or three-peak features at high biases, where additional peaks appear at large-current locations. On the other hand, histograms of the magnitude of the current on the wetting layers exhibit the same single-peak feature for all biases. This indicates the conductive mechanism is significantly different for QDs and wetting layers. While the small-current peak of QDs can be attributed to the Fowler–Nordheim tunneling model at low biases and the Schottky emission model at high biases respectively, the large-current peak(s) may be attributed to the discrete energy levels of QDs. The results suggest the conductive mechanisms of GeSi QDs can be regulated by the applied bias.

1. Introduction

Self-assembled GeSi quantum dots (QDs) have been the subject of intensive studies over recent decades due to their potential applications in Si-based quantum electronics [1, 2]. Previous investigations of the electrical properties of GeSi QDs have usually been concentrated on the ensemble of QDs by various ways, such as capacitance spectroscopy, deep level transient spectroscopy and admittance spectroscopy [3–5]. However, those researches may not be precisely adequate to understand the QDs' electrical properties due to the large scatter in size, composition distribution and so on.

Regarding to the electrical studies on individual QDs, a sensitive and high spatial resolution technology is required. Fortunately conductive atomic force microscopy (CAFM)

offers an effective way to study the conductive properties of individual QDs [6–8], which have already been employed on various QDs, including GeSi [9, 10], GaN [11, 12], InP [13], TiSi₂ [14], and so on.

Although GeSi QDs have been explored both experimentally and theoretically, their electrical properties are still not well understood because the complexities of the composition and morphology of the QD involved in the GeSi system [15, 16]. In our previous work, we have used CAFM to study the electrical properties of individual GeSi QDs by current image characteristics and suppose a possible conductive model [17, 18]. However the influence of the applied bias on the current distribution is less concerned in the CAFM measurements. Almost all existing studies give current distributions of QDs at a fixed bias, and few reports [19] have discussed the dependence of QDs' current distributions on the applied bias.

³ Author to whom any correspondence should be addressed.

In this work, the current distributions of individual self-assembled GeSi QDs are studied as a function of bias by using CAFM. By analyzing the bias-dependent current images of GeSi QDs and statistic histograms of the current magnitude at different biases, the conductive mechanisms for QDs and for wetting layers are supposed. The results reveal that the current distribution of GeSi QDs can be regulated by the applied bias.

2. Experimental details

The GeSi QDs used for CAFM measurements are fabricated on a p-type Si(100) substrate (1–10 Ω cm) by molecular beam epitaxy. First a 50 nm Si buffer layer was deposited and then a 0.75 nm Ge was grown at 640 °C [20]. After the growth the sample was kept at 640 °C for several minutes before it was cooled down to room temperature naturally.

All CAFM measurements were performed by a commercial AFM (Sloer P47, NT-MDT) with a Pt-coated conductive tip in contact mode at room temperature. All topographic and current images were simultaneously obtained under a flowing dry nitrogen atmosphere, allowing a direct correlation between the conductance properties and surface morphology with high lateral resolution. During measurements the tip was grounded while the bias was applied on the sample.

It was observed that sample oxidation is serious for positive sample bias, where a much smaller or even no current could be measured in the second scan. But for the negative sample bias, the current image of GeSi QDs can be measured several times, indicating the oxidation is reduced at negative sample biases. Therefore in this paper, all the current images were measured at negative sample biases. Furthermore, to avoid any possible effects induced by the former scan, a fresh area was selected for every couple of height and current image measurements. To avoid the fluctuation of results on different QDs, statistical histograms of current magnitude were calculated for all biases. Each histogram is calculated by using a whole current image (256 pixels \times 256 pixels) with a size of 1 $\mu\text{m} \times 1 \mu\text{m}$ and converting all data to the matrix. The data of QDs and wetting layers are distinguished according to the corresponding height value from the topographic image obtained simultaneously with the current image. The peak current of the histogram was obtained by the numerical fitting method with log-normal distribution [21].

3. Results and discussion

The topographic and current images of self-assembled GeSi QDs measured at different biases from -0.5 to -2 V are shown in figure 1. The topographic images showed that the GeSi QDs are dome-shaped with an average diameter of 100 nm and height of 15 nm. From the current images, a ring-shaped current distribution of individual QDs can be observed for all four biases. When the bias varies from -0.5 to -2 V, the conductivity of the periphery of the GeSi QDs is always higher than that of the center, and the current distribution does not show an obvious change with the bias. The typical current profiles across individual QDs at four biases are shown in the right column of figure 1. It shows the same dual-peak feature,

confirming that the characteristics of current distribution did not change as the bias varied from -0.5 to -2.0 V, while the magnitude of current gradually increased. The current profiles are also made on different QDs as well as along the different directions of the same QD for four biases; the same dual-peak feature can be observed. Therefore within the bias range of -0.5 to -2.0 V, the periphery of GeSi QDs always shows better conductivity than that of the central part. The ring-shaped current distribution was interpreted in our previous paper [9]. The main point is that the ring-shaped current distribution is mainly attributed to the high Si-alloyed GeSi composition uniformly distributed in QDs and also the topographic shape effect.

On the contrary, the current distributions of QDs obtained at high biases show significantly different features. The topographic and current images of GeSi QDs obtained at biases ranging from -2.5 to -4.0 V are shown in figure 2. From the current images, all the current distributions of individual QDs are in a disc-like shape, which is totally different from the ring-like shape under the low biases. The current intensity enhances sharply as the bias magnitude increases, and the central parts of QDs become more conductive than the other ones. Current profiles are made on many individual QDs as well as along different directions of the same QD, and four typical current profiles for four biases are shown in the right column of figure 2. All current profiles of GeSi QDs obtained at the high biases yield similar dome-shape characteristics, except a little current magnitude increase and shape broadening with increasing bias magnitude. At the bias of -4 V, the top of the QD current profile is somewhat flattened at about -30 nA, which is caused by the saturation limitation of the instrument.

To analysis the bias-dependent conductance distribution of QDs in detail, the statistical distributions of current magnitude have been calculated. Histograms of the current magnitude derived from the current on a number of QDs and wetting layers regions at biases ranging from -0.5 to -4 V are presented in figure 3 and figure 4, respectively. In figure 3, the current histograms of QDs under biases from -0.5 to -2 V show similar features, i.e. a single peak located at the small-current region. As the bias varies from -0.5 to -2 V, the magnitude of peak current increases from 7.2 to 14.3 pA, and the current range broadens while the count number of the peak decreases. On the other hand, the statistic histograms of current images obtained at biases ranging from -2.5 to -4 V display obviously different characteristics. Except the same small-current peak as obtained at low biases, one or two additional peaks appeared at the large-current region(s). The peak current of the novel peak is about -25 nA at the bias of -3 V. Combined with the dome-shaped current profile, the novel peak should be attributed to the high conductance of the QDs' central part. Further increasing the bias to -4 V, a second novel peak appears at about -30 nA in the current histogram. The shape of the current peak is sharper at the large-current side, which may be induced by the limitation of current saturation.

For comparison, the statistics histograms of current magnitude derived from the wetting layers at biases ranging from -0.5 to -4 V are shown in figure 4. All current

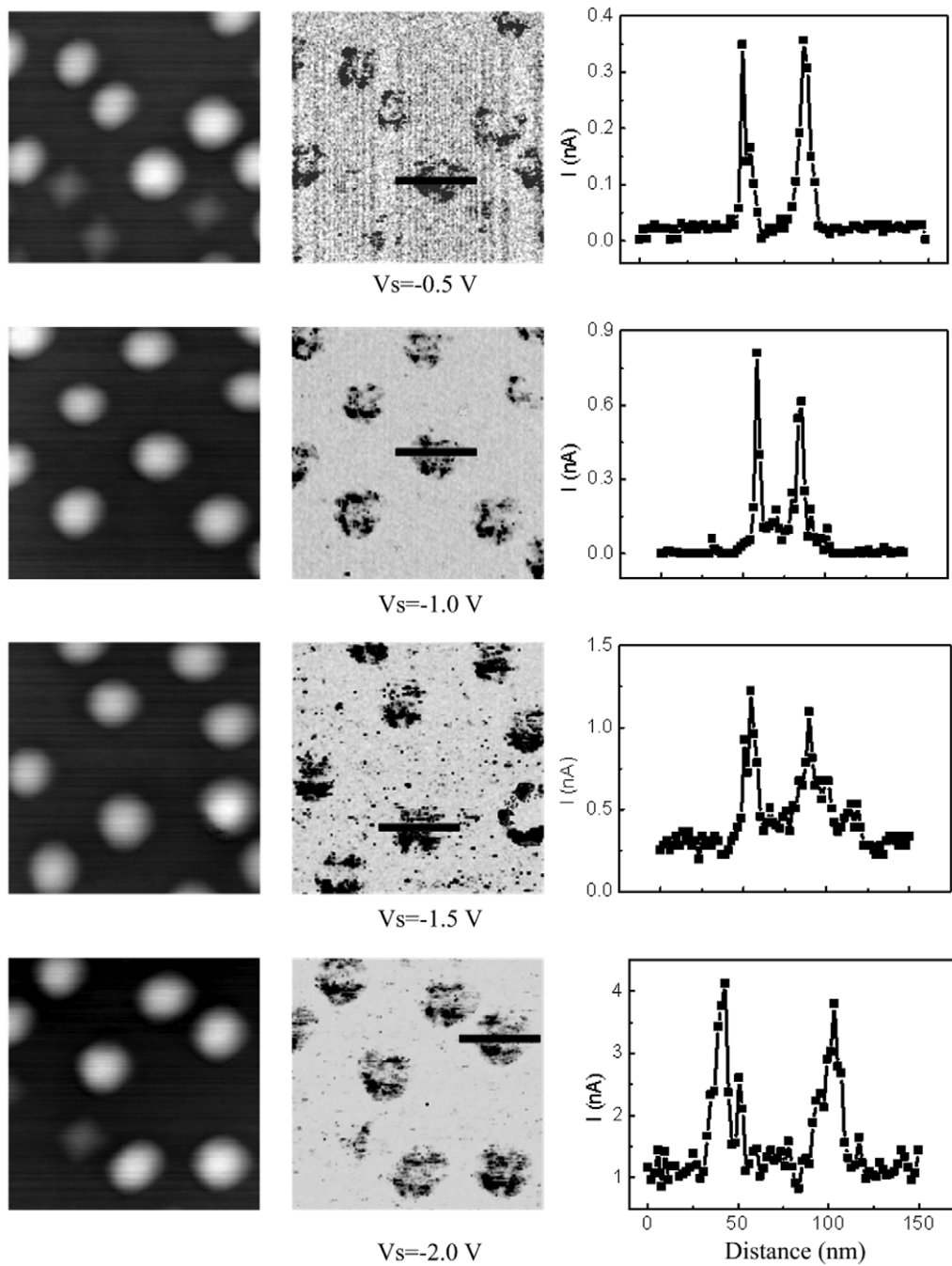


Figure 1. The topographic (left column) and current (middle column) images of GeSi QDs measured at biases from -0.5 to -2 V. The images size is $0.5 \mu\text{m} \times 0.5 \mu\text{m}$. Profile lines across individual QDs as marked in current images are shown in the right column.

histograms of the wetting layers show a similar single-peak feature, where only one peak appears at the small-current region. As the bias magnitude increases, the feature of the peak shape shows no obvious change, except an inconspicuous peak broadening and peak current shift. From the above results, it can be indicated that novel large-current peak(s) of QDs should be related to the quantum effects of quantum dots, i.e. discrete energy levels in quantum dots.

To understand the conductive mechanism of quantum dots and wetting layers, the dependence of the peak current on the bias was investigated. The peak current value I_0 of the histogram peak located at small-current region was obtained

by a log-normal distribution fitting [21] as follows:

$$n(I) = \frac{A}{\sqrt{2\pi}\sigma I} e^{-[\ln(I) - \ln(I_0)]^2 / 2\sigma^2} \quad (1)$$

where I_0 is the histogram peak position, A is a normalization factor, and σ is the variance. The fitting results for QDs and for wetting layers are given in figure 5. For the wetting layers, the dependence of the peak current on the bias ($I_0 \sim V$) can be well fitted by the Fowler–Nordheim (FN) tunneling mode [22, 23] for the all biases, plotted as the solid line in figure 5(b). On the other hand, for the QDs, the dependence of current peak I_0 on applied bias V agrees with the FN

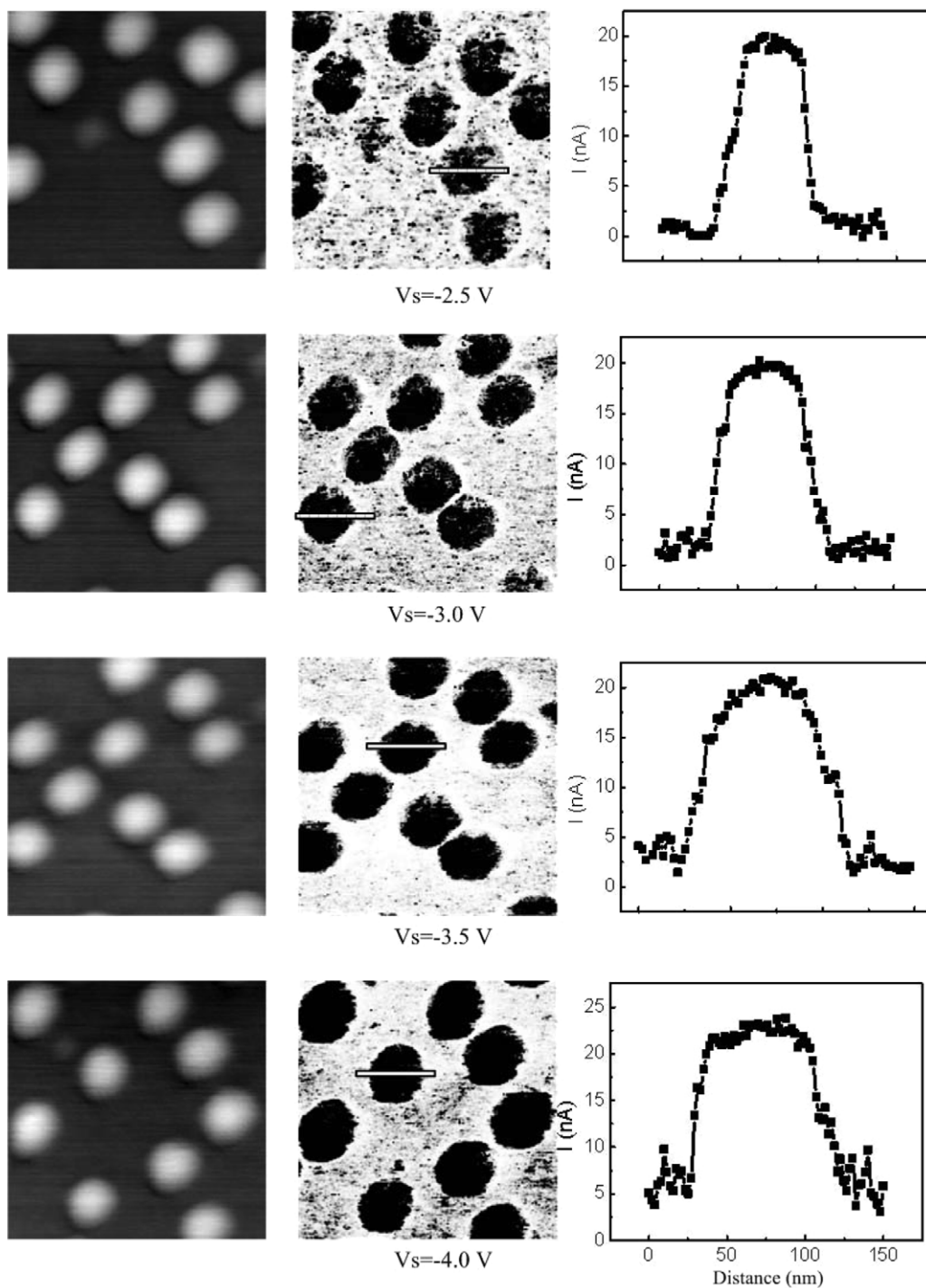


Figure 2. The topographic (left column) and current (middle column) images as well as profile lines (right column) of GeSi QDs measured at biases from -2.5 to -4 V. The image size is $0.5 \mu\text{m} \times 0.5 \mu\text{m}$.

tunneling mode under low biases and the Schottky emission (SE) model [24] under high biases. The histogram peaks located at the large-current regions are also fitted by a log-normal distribution. However, the dependence of the peak current on the bias does not obey the FN tunneling nor the Schottky emission model.

From the above statements, the conductive mechanism of the wetting layers can be simply determined by FN tunneling for all biases. However, for QDs one of the contributions to

the conductance can be due to FN tunneling at low biases and Schottky emission at high biases respectively, and this contribution can be regulated by the applied bias. The other contribution is the unclear factor which resulted in the large-current peak(s). It may be attributed to the direct transfer of the electrons and/or holes via the discrete energy levels in QDs. In a previous paper, Johal *et al* calculated tunneling current spectra for different locations in the InGaAs QDs for a series of biases [19]. They found at a low bias of -0.53 eV the

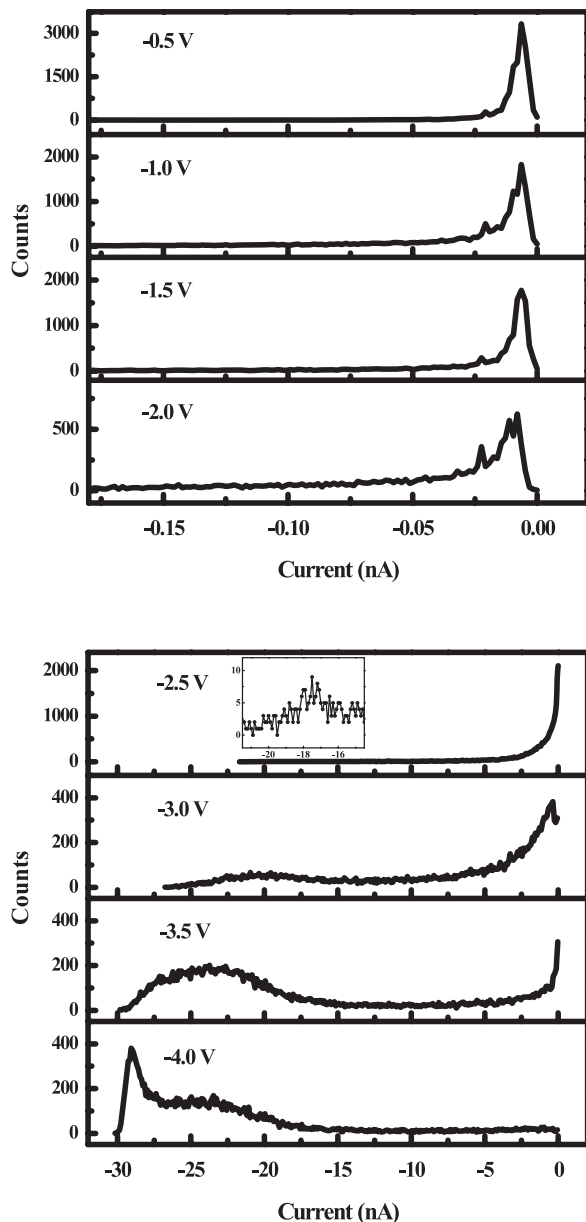


Figure 3. Histograms of current magnitude derived from a number of GeSi QDs at biases ranging from -0.5 to -4.0 V.

contribution to the tunneling current is due solely to the $1s$ -like state which is spherically symmetric and gives rise to the tunneling current at the center of the QD. With increasing bias, higher level eigenstates contributed to the tunneling current, resulting in the spread of the current at the center of the QD to the periphery of the QD. The calculation explained the spatial tunneling current distribution of InGaAs QDs at various biases obtained by STM in UHV. A similar mechanism may be able to roughly explain the bias-dependent current distributions of GeSi QDs. As the bias increases above a certain value, the current at the QDs center increases much faster than the periphery since more eigenstates localized at the QDs center contribute to the current. The larger biases needed in our case may be due to the existence of an oxide layer and/or space charge layer. However, a complete understanding

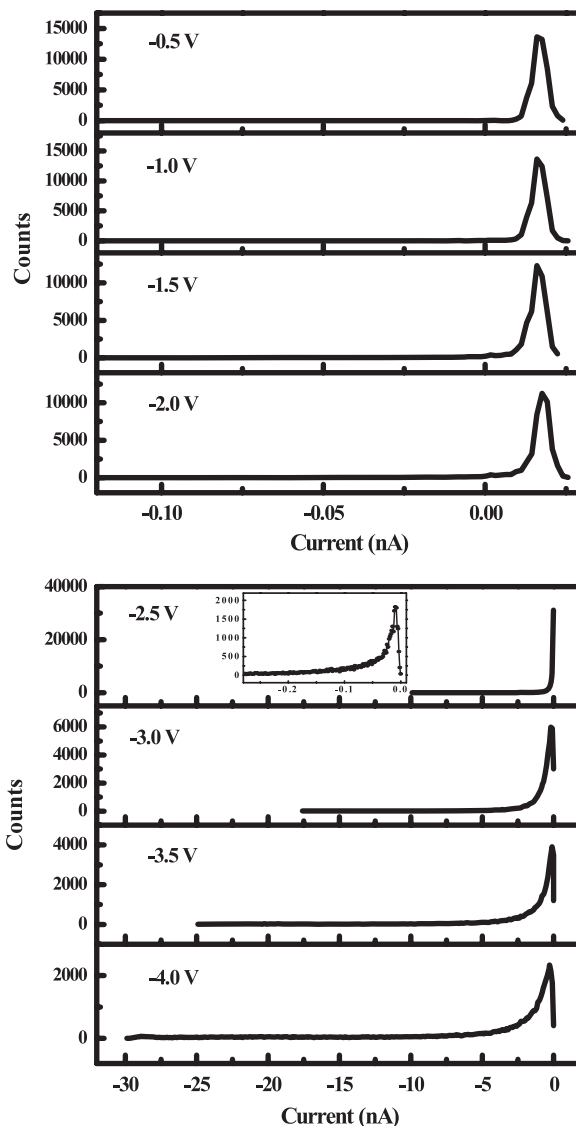


Figure 4. Histograms of current magnitude derived from wetting layers at biases ranging from -0.5 to -4.0 V.

of the mechanism is yet to be developed, by including all contributions of the oxide layer, space charge, surface states, and so on.

4. Conclusion

In summary, the topography and electrical properties of GeSi QDs have been probed by conductive atomic force microscopy. Our studies show that the current distributions of GeSi QDs vary with the applied bias. At low biases, only the periphery parts of QD are conductive and only one current peak is exhibited in the statistics histograms of current magnitude, while at high biases the center parts of GeSi QDs show higher conductive characteristics, and novel peaks corresponding QDs center parts can be distinguished in the statistics histograms. The conductive mechanism of QDs should have two contributors. One is FN tunneling at low biases and Schottky emission at high biases, and the other may

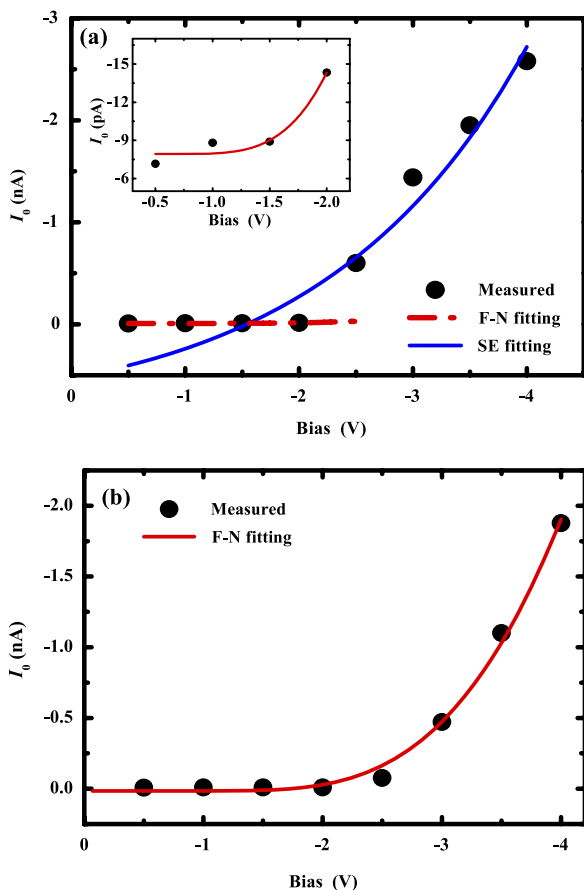


Figure 5. The peak current of QDs (a) and wetting layers (b) as a function of sample bias. The fitting curves are shown as lines. The inset in figure 5(a) is zoomed to show the FN fitting at low biases. (This figure is in colour only in the electronic version)

be due to the discrete energy level of QDs. On the contrary, the conductive mechanism of the wetting layers can be simply attributed to FN tunneling.

Acknowledgments

This work was supported by the National Natural Science Foundation of China (Grant number 10874030), and partially supported by the Shanghai Science and Technology

Commission (No. 08ZR1401200) and the special funds for Major State Basic Research Project of China (No. 2011CB925601).

References

- [1] Kiravittaya S, Rastelli A and Schmidt O G 2009 *Rep. Prog. Phys.* **72** 046502
- [2] Tsybeskov L and Lockwood D J 2009 *Proc. IEEE* **97** 1284
- [3] Suganuma Y, Trudeau P E and Dhirani A A 2002 *Phys. Rev. B* **66** 241405
- [4] Zhang S K, Zhu H J, Lu F, Jiang Z M and Wang X 1998 *Phys. Rev. Lett.* **80** 3340
- [5] Cai X S, Qin J, Yang H B, Yuan F Y, Fan Y L, Lu F and Jiang Z M 2006 *Appl. Surf. Sci.* **252** 2776
- [6] Stomp R, Miyahara Y, Schaer S, Sun Q, Guo H, Grutter P, Studenikin S, Poole P and Sachrajda A 2005 *Phys. Rev. Lett.* **94** 056802
- [7] Bari M R, Blaikie R J, Fang F and Markwitz A 2009 *J. Vac. Sci. Technol. B* **27** 3051
- [8] Troyon M and Smaali K 2008 *Nanotechnology* **19** 255709
- [9] Xue F, Qin J, Cui J, Fan Y L, Jiang Z M and Yang X J 2005 *Surf. Sci.* **592** 65
- [10] Chung H C, Chu W H and Liu C P 2006 *Appl. Phys. Lett.* **89** 082105
- [11] Leconte S, Guillot F, Sarigiannidou E and Monroy E 2007 *Semicond. Sci. Technol.* **22** 107
- [12] Spradlin J, Doğan S, Xie J, Molnar R, Baski A A and Morkoc H 2004 *Appl. Phys. Lett.* **84** 4150
- [13] Vicaro K O, Cotta M A, Gutiérrez H R and Bortoleto J R R 2003 *Nanotechnology* **14** 509
- [14] Tanaka I, Kamiya I, Sakaki H, Qureshi N, Allen S J and Petroff P M 1999 *Appl. Phys. Lett.* **74** 844
- [15] Azulay D, Balberg I, Chu V, Conde J P and Millo O 2005 *Phys. Rev. B* **71** 113304
- [16] Tokar D, Balberg I, Zelaya-Angel O, Savir E and Millo O 2006 *Phys. Rev. B* **73** 045317
- [17] Wu R, Li F H, Jiang Z M and Yang X J 2006 *Nanotechnology* **17** 5111
- [18] Wu R, Li J H, Zhang S L, Yang H B, Jiang Z M and Yang X J 2008 *Chin. Phys. Lett.* **25** 4360
- [19] Johal T K, Rinaldi R, Passaseo A, Cingolani R, Vasanelli A, Ferreira R and Bastard G 2002 *Phys. Rev. B* **66** 075336
- [20] Wu Y Q, Li F H, Cui J, Lin J H, Wu R, Qin J, Zhu C Y, Fan Y L, Yang X J and Jiang Z M 2005 *Appl. Phys. Lett.* **87** 223116
- [21] Schaadt D M, Yu E T, Vaithyanatan V and Schlom D G 2004 *J. Vac. Sci. Technol. B* **22** 2030
- [22] Frammelsberger W, Benstetter G, Stamp R, Kiely J and Schweinboeck T 2005 *Mater. Sci. Eng. B* **116** 168
- [23] Xie X N, Chung H J, Sow C H and Wee A T S 2004 *Appl. Phys. Lett.* **84** 4914
- [24] Oh J and Nemanich R J 2002 *J. Appl. Phys.* **92** 3326